Economic Friendly ZnO-Based UV Sensors

Subjects: Materials Science, Biomaterials

Contributor: Liguo Qin

Ultraviolet (UV) sensors offer significant advantages in human health protection and environmental pollution monitoring. Amongst various materials for UV sensors, the zinc oxide (ZnO) nanostructure is considered as one of the most promising candidates due to its incredible electrical, optical, biomedical, energetic and preparing properties. Compared to other fabricating techniques, hydrothermal synthesis has been proven to show special advantages such as economic cost, low-temperature process and excellent and high-yield production.

zinc oxide nanostructures | hydrothermal | localized heat growth | seed patterned growth | growth critical parameters | UV sensors

1. Introduction

Ultraviolet (UV) light provides a special benefit on the well-being of humans by killing microorganisms. However, higher exposure has been reported to cause side effects such as skin cancer, cataracts or immune system suppression. Therefore, sensors that possess the ability of efficiently detecting UV signals have attracted huge attention [1][2][3]. These UV sensors were divided into two groups, including vacuum UV sensors and solid-state UV sensors [4][5][6]. Vacuum UV sensors are based on photomultiplier tubes and their derived devices, whereas solid-state UV sensors are based on semiconductor materials [4]. Compared to solid-state UV sensors, vacuum UV sensors have some disadvantages such as large size, high power consumption, low quantum efficiency, high pressure, low-temperature working conditions and high cost [7]. Therefore, solid-state UV sensors are the new focus for UV technology [4][8][9][10][11].

In the last few decades, semiconducting metal oxide nanoscale materials were the most likely candidates for electronic, optical, biomedical and thermal applications. They were widely used in UV lasers, sensors, field-effect transistors, field emission devices, energy harvesters, light-emitting sources, phonic devices and nanogenerators [3][4][12][13][14][15][16][17][18][19][20][21][22]. These metal oxide materials include zinc oxide (ZnO), nickel oxide (NiO), titanium oxide (TiO 2), copper oxide (CuO), tin oxide (SnO 2), iron oxide (Fe 2O 3), indium oxide (In 2O 3), tungsten trioxide (WO 3) and vanadium oxide (V 2O 3) [1][4][14][17][19][23][24][25][26][27][28]. Among all of these materials, ZnO has gained considerable interest due to its fascinating unique properties, as mentioned in **Table 1** . Its properties include a direct large bandgap (3.37 eV), huge excitation binding energy (60 meV), excellent electron mobility (1 to 200 cm 2/V. s) and huge piezoelectric coefficient (d 33~12 pm/V) [13][16][17][23][29][30][31]. Excellent biocompatibility, biodegradability and chemical stability, as well as amazing electrical and optical properties are also some great characteristics of ZnO [12][13][15][17][20][25][32][33]. Meanwhile, various morphologies of ZnO

nanomaterials have been investigated, such as nanoparticles, nanowires, nanoneedles and nanotubes, which accordingly expand their applications in various fields [12][13][14][17][19][34].

Table 1. Summary of ZnO nanostructure properties.

Type of Property	Property
Preparation	Easy to grow [12]. Low- and high-temperature operation capability. Architecture and property controllability. Facility of integration on either rigid or flexible devices [20].
Optical	Large bandgap [13]. Good transparency to visible light. Luminescent material [20]. Good transmissibility and reflexibility [35][36].
Electrical	Semiconductor material. Good electron mobility [37]. Good chemical stability [16]. Huge piezoelectric coefficient [11][38].
Biomedical	Excellent biocompatibility [13][20]. Excellent biodegradability [25]. Non-toxicity [33][37].
Energy	Huge excitation binding energy [16][23]. Photocatalytic material [37][39].

ZnO is available in three crystalline structures, including wurtzite, zinc blende and rock salt. Wurtzite structure is a two-lattice parameter-based hexagonal unit cell with a = 0.3296 nm and c = 0.52065 nm [13][18][40]. ZnO wurtzite is stable under ambient conditions, but it is transformed into rock salt at relatively high pressure (approximately 10 GPa) [18][41]. The zinc blende can only be obtained at its stable phase on cubic substrates [20][41].

Recently, comprehensive work was reported in synthesizing ZnO nanostructures for UV sensors [4][40][42]. Their majority was focusing on various synthesis methods. However, each method possesses various approaches and it was short of a detail interpretation about the mechanism of each method. As economic cost for the synthesis is under increasing challenge, a comprehensive review on each method is of great importance for the future study. To the best of authors' knowledge, no previous review has precisely examined all of hydrothermal approaches and summarized the effect of critical parameters on the ZnO synthesis. Therefore, the current review aims on the latest approaches of ZnO hydrothermal growths and the effect of different parameters on its morphology. This paper provides an overview of the recent developments in ZnO nanostructure synthesis for UV sensors, particularly the hydrothermal synthesis. Different hydrothermal approaches are compared, and the critical parameters are discussed in detail. Lastly, the hydrothermal ZnO-based UV sensors for UV light are discussed as well. This review may provide a better comprehension of the current research status for hydrothermal ZnO-based applications.

2. ZnO Nanostructures' Hydrothermal Growth

ZnO is a fascinating material with various morphologies. The chemical and physical characteristics vary as a function of morphology, size, shape and crystalline structures. Previous works have demonstrated that this material can be modelled on the desired shape and size [12][14][17][18][43][44].

Hydrothermal method is carried out in an aqueous solution by an autoclave system [2][33][34][37][41]. It contains two typical steps as illustrated in **Figure 1** .

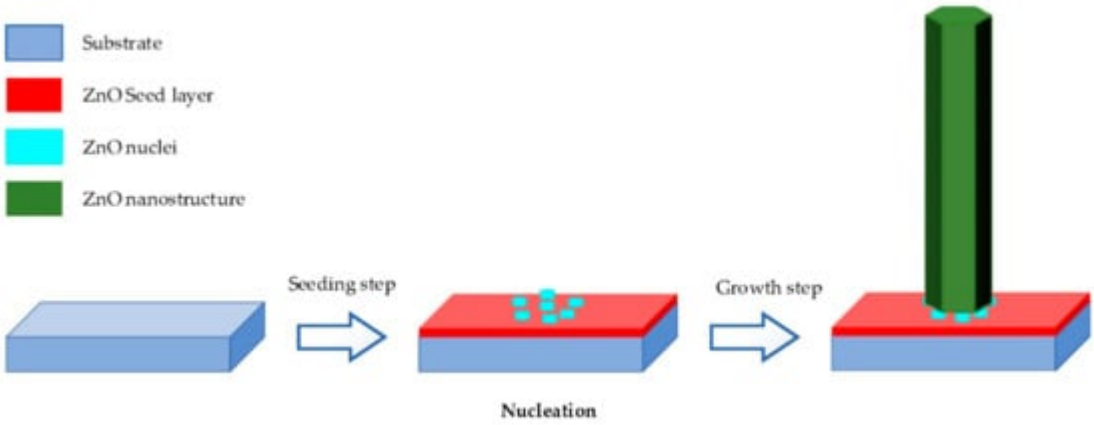

Figure 1. Diagram of hydrothermal process, reproduced with permission from Reference [2].

- Seeding: The subtract is seeded with a layer of ZnO nanoparticles. The seeded nanoparticles play a role in promoting nucleation for nanostructure growth by decreasing the thermodynamic barrier. The less the nucleation of ZnO is, the bigger ZnO growth and the better the crystallinity of ZnO [45].

- Growing: The seeded subtract is kept in the precursor at a certain temperature for a fixed period to ensure stable growing regimes. The precursor is a mixture of aqueous solutions containing alkaline reagent (such as NaOH, KOH and hexamethylenetetramine (HMTA)) and zinc ion salt (such as Zn $(NO_3)_2$ and $ZnCl_2$) [39][40][46][47]. In addition to the precursor, a guiding agent (such as polyethyleneimine (PEI)) is inserted to decrease the lateral growth and maximize the length of nanostructures.

Deng et al. employed the hydrothermal process to grow ZnO nanorods on flexible Kapton substrate at low temperature with an equimolar solution of HMTA and zinc nitrate hexahydrate as a precursor [19]. They obtained nanorods in the form of regular hexagonal prisms with a length of 60 nm and a diameter of 100 nm. Vijayakumar et al. presented ZnO nanotubes synthesized by hydrothermal method in autoclave for 4 h at 90 °C for CO gas sensing [48]. Hu et al. hydrothermally synthesized ZnO nanowires on polyethylene terephthalate (PET) fabrics at 95 °C for 4 h [34]. The as-grown nanowires were treated hydrophobically by polydimethylsiloxane (PDMS) for lotus effect. Via hydrothermal growth, Wu et al. demonstrated the synthesis of graphene quantum dot doped ZnO superstructures for weak UV intensity sensor application at 90 °C for 2 h [49].

In order to control the morphology, orientation, aspect ratio and surface density of the ZnO nanostructure, parameters involved in the process must be optimized. Examples of parameters affecting nanostructure growth morphology are the pH of the solution, reagents, seed layers, temperature, guiding agents, growth time and mechanical agitations [18][50].

3. Influence of Fabrication Parameters on ZnO Hydrothermal Growth

With cautious adding ammonium hydroxide NH 4OH in the precursor mixture, Boubenia et al. discovered a possibility of enhancing the nucleation sites, which led to the control of nanowires' electrical properties and expanded the applications for flexible and electromechanical devices [16]. Based on their work, they explained the density-controlled synthesis growth mechanism of ZnO nanowires as follows: The amount of NH 4OH had a straight effect over the concentration of Zn (II) complexes, which would significantly impact the Zn solubility in the solution. Thus, the supersaturation of precursor solution was controlled as well as the quantity of nuclei over the target substrate.

In hydrothermal growth process, growth time is another important critical parameter of ZnO nanostructures [51][52][53][54][47]. As shown in **Table 2** , researchers fabricated ZnO nanostructures with different growth times to set up the relationship between yield of growth and their morphologies.

Table 2. Advantages and disadvantages of selective hydrothermal growths.

ZnO Morphology	Starting Materials	Synthesis Temperature (°C)	Growth Time	Diameter of ZnO Nanostructures	Length of ZnO Nanostructures	References
Nanowires	25 mM of zinc nitrate hexahydrate, 25 mM HMTA and 5–7 mM PEI.	95	1 h	200–400 nm	10–12 µm	[55]
Nanowires	25 mM of zinc nitrate hexahydrate, 25 mM HMTA, 5–7 mM PEI and deionized (DI) water.	95	1 h	>20 µm	-	[56]
Nanowires	25 mM of zinc nitrate hexahydrate, 25 mM HMTA and 6 mM PEI.	-	-	-	9.9 µm	[24]
Nanowires	25 mM of zinc nitrate hexahydrate, 25 mM	90	2.5 h	100–150 nm	1–3 µm	[57]

ZnO Morphology	Starting Materials	Synthesis Temperature (°C)	Growth Time	Diameter of ZnO Nanostructures	Length of ZnO Nanostructures	References
	HMTA and 5–7 mM PEI.					
Nanowires	25 mM of zinc nitrate hexahydrate, 25 mM HMTA and 5–7 mM PEI.	95	1 h	15 µm	200–400 nm	[58]
Hemispherical bumps	Mixture of equimolar zinc nitrate hexahydrate and HMTA.	90	5 h	400 nm	2.2 µm	[59]
Nanorods	Mixture of equimolar zinc nitrate hexahydrate and HMTA.	90	3 h	100 nm	800 nm	[60]
Nanorods	50 mL of solution containing 0.1 M zinc nitrate hexahydrate, 0.1 M HMTA and DI water.	90	2 h	70 nm	15 µm	[26]
Nanorods	Mixture of equimolar zinc nitrate hexahydrate and HMTA	90	4 h	1.2	-	[2]
Flower-like structure	Zinc acetate dehydrate and NaOH.	120	15 min	0.6 µm	5.2 µm	[32]
Nanowires	$ZnCl_2$. $NaCO_3$ and DI water.	140	6 h	50 nm	1 µm	[52]
Vertical aligned nanorods	$Zn(CH_3COO)_2{\cdot}2H_2O$, HMTA, absolute ethanol and distilled water.	400	-	50 nm	500 nm	[13]
Nanorods	10 mL $Zn(Ac)_2.2H_2O$ in 0.1 M methanol, 20 mL NaOH in 0.5 M methanol, DI water (K_2SnO_3,$3H_2O$, 95%), 0.75 g of urea.	150	24 h	2.8 nm	26 nm	[43]

ZnO Morphology	Starting Materials	Synthesis Temperature (°C)	Growth Time	Diameter of ZnO Nanostructures	Length of ZnO Nanostructures	References
	20 mM $Zn(NO_3)_2$ and 20 mM HMTA	90 °C for 100 min, dried for 12 h at 60 °C and annealed 1 h at 500°C.	-	290–330 nm	3.2–3.4 µm	

-: Not reported.

The type of synthesized ZnO nanostructures is also affected by the temperature. On the Zn foil substrate, Lu et al. synthesized well-aligned ZnO nanorods of 30 nm in diameter and 200 nm in length at 22 °C and ultralong ZnO nanowires arrays with honeycomb-like structures of 60 to 200 nm in diameter and 10 to 30 mm in length at elevated temperature under similar conditions [61].

In hydrothermal method, ZnO nanostructures were treated with thermal annealing after either the seed deposition or the growth in order to alter their properties [1][60][62][63]. For instance, Filip et al. reported a significant difference in crystalline structure on a seed layer between annealed and non-annealed substrates [35]. Lupan et al. demonstrated that post-treatment thermal annealing led to improvement in the crystallinity and the performance of ZnO nanomaterials [64]. Sandeep Sanjeev and Dhananjaya Kekuda also showed that annealing temperature affected the structural and optical properties of the ZnO thin film [36]. Wahid et al. reported that the optimum annealing temperature was 150 °C, where they obtained high-resistant ZnO nanorods with a length and diameter of 4000 nm and 379 nm, respectively [65]. They also discovered that the ZnO growth rate depended on the annealing temperature, as vertical nanorods were observed below 150 °C and ZnO homocentric bundles on the vertical nanorods above 150 °C. Through careful analysis of the seed layer, Wahid et al. explained the mechanism behind this observation as follows. At annealing temperatures above 150 °C, more energy was present in the seed layer, which enhanced the kinetic energy of the seed layer molecule. In consequence, the molecular motion increased and this caused the seed layer to stretch more and reduce the surface tension. As a result, the seed nanoparticles agglomerated, which then brought the nanoparticles together during the annealing process. As the seed nanoparticles were agglomerating, the active nucleation sites of ZnO seed were disorientated, resulting in multifarious ZnO nanorod growth orientation, which promoted bundling of the ZnO nanorods [65][66]. Meanwhile, Wei et al. reported that this agglomeration phenomenon happened because annealing produced the dried organic compound (diethanolamine) [67].

References

1. Ozel, K.; Yildiz, A. SnO2/ZnO/p-Si and SnO2/TiO2/p-Si heterojunction UV photodiodes prepared using a hydrothermal method. Sens. Actuators A Phys. 2020, 315, 112351.

2. Asib, N.A.M.; Husairi, F.S.; Eswar, K.A.; Afaah, A.N.; Mamat, M.H.; Rusop, M.; Khusaimi, Z. Developing high-sensitivity UV sensors based on ZnO nanorods grown on TiO2 seed layer films using solution immersion method. Sens. Actuators A Phys. 2020, 302, 111827.
3. Zou, W.; González, A.; Jampaiah, D.; Ramanathan, R.; Taha, M.; Walia, S.; Sriram, S.; Bhaskaran, M.; Dominguez-Vera, J.M.; Bansal, V. Skin color-specific and spectrally-selective naked-eye dosimetry of UVA, B and C radiations. Nat. Commun. 2018, 9, 3743.
4. Zou, Y.; Zhang, Y.; Hu, Y.; Gu, H. Ultraviolet detectors based on wide bandgap semiconductor nanowire: A review. Sensors 2018, 18, 2072.
5. Razeghi, M.; Rogalski, A. Semiconductor ultraviolet detectors. J. Appl. Phys. 1996, 79, 7433–7473.
6. Shi, L.; Nihtianov, S. Comparative study of silicon-based ultraviolet photodetectors. IEEE Sens. J. 2012, 12, 2453–2459.
7. Shen, T.; Dai, X.; Zhang, D.; Wang, W.; Feng, Y. ZnO composite graphene coating micro-fiber interferometer for ultraviolet detection. Sensors 2020, 20, 1478.
8. AlZoubi, T.; Qutaish, H.; Al-Shawwa, E.; Hamzawy, S. Enhanced UV-light detection based on ZnO nanowires/graphene oxide hybrid using cost-effective low temperature hydrothermal process. Opt. Mater. 2018, 77, 226–232.
9. Liu, Y.; Song, Z.; Yuan, S.; Xu, L.; Xin, Y.; Duan, M.; Yao, S.; Yang, Y.; Xia, Z. Enhanced Ultraviolet Photodetection Based on a Heterojunction Consisted of ZnO Nanowires and Single-Layer Graphene on Silicon Substrate. Electron. Mater. Lett. 2020, 16, 81–88.
10. Rai, S.C.; Wang, K.; Ding, Y.; Marmon, J.K.; Bhatt, M.; Zhang, Y.; Zhou, W.; Wang, Z.L. Piezophototronic Effect Enhanced UV/Visible Photodetector Based on Fully Wide Band Gap Type-II ZnO/ZnS Core/Shell Nanowire Array. ACS Nano 2015, 9, 6419–6427.
11. Kou, L.Z.; Guo, W.L.; Li, C. Piezoelectricity of ZnO and its nanostructures. In Proceedings of the 2008 Symposium on Piezoelectricity, Acoustic Waves, and Device Applications, Nanjing, China, 5–8 December 2008; pp. 354–359.
12. Kang, Y.; Yu, F.; Zhang, L.; Wang, W.; Chen, L.; Li, Y. Review of ZnO-based nanomaterials in gas sensors. Solid State Ion. 2021, 360, 115544.
13. Ditshego, N.M.J. ZnO nanowire field effect transistor for biosensing: A review. J. Nano Res. 2019, 60, 94–112.
14. Şerban, I.; Enesca, A. Metal Oxides-Based Semiconductors for Biosensors Applications. Front. Chem. 2020, 8, 354.
15. Characterization of Zinc Oxide Nanorod. Available online: https://www.azonano.com/article.aspx?ArticleID=2509 (accessed on 15 May 2021).

16. Boubenia, S.; Dahiya, A.S.; Poulin-Vittrant, G.; Morini, F.; Nadaud, K.; Alquier, D. A facile hydrothermal approach for the density tunable growth of ZnO nanowires and their electrical characterizations. Sci. Rep. 2017, 7, 369.
17. Xu, S.; Wang, Z.L. One-dimensional ZnO nanostructures: Solution growth and functional properties. Nano Res. 2011, 4, 1013–1098.
18. Galdámez-Martinez, A.; Santana, G.; Güell, F.; Martínez-Alanis, P.R.; Dutt, A. Photoluminescence of ZnO nanowires: A review. Nanomaterials 2020, 10, 857.
19. Rong, P.; Ren, S.; Yu, Q. Fabrications and Applications of ZnO Nanomaterials in Flexible Functional Devices-A Review. Crit. Rev. Anal. Chem. 2019, 49, 336–349.
20. Bagga, S.; Akhtar, J.; Mishra, S. Synthesis and applications of ZnO nanowire: A review. In AIP Conference Proceedings; AIP Publishing LLC.: Melville, NY, USA, 2018; Volume 1989.
21. Bhati, V.S.; Hojamberdiev, M.; Kumar, M. Enhanced sensing performance of ZnO nanostructures-based gas sensors: A review. Energy Rep. 2020, 6, 46–62.
22. Xie, Y.; Yang, S.; Mao, Z.; Li, P.; Zhao, C.; Cohick, Z.; Huang, P.-H.; Huang, T.J. In Situ Fabrication of 3D Ag @ ZnO Nanostructures for Micro fl uidic. ACS Nano 2014, 8, 12175–12184.
23. Humayun, Q.; Kashif, M.; Hashim, U.; Qurashi, A. Selective growth of ZnO nanorods on microgap electrodes and their applications in UV sensors. Nanoscale Res. Lett. 2014, 9, 29.
24. Yang, D.; Kim, D.; Ko, S.H.; Pisano, A.P.; Li, Z.; Park, I. Focused energy field method for the localized synthesis and direct integration of 1D nanomaterials on microelectronic devices. Adv. Mater. 2015, 27, 1207–1215.
25. Beitollahi, H.; Tajik, S.; Garkani Nejad, F.; Safaei, M. Recent advances in ZnO nanostructure-based electrochemical sensors and biosensors. J. Mater. Chem. B 2020, 8, 5826–5844.
26. Noothongkaew, S.; Thumthan, O.; An, K.S. UV-Photodetectors based on CuO/ZnO nanocomposites. Mater. Lett. 2018, 233, 318–323.
27. Paeng, D.; Lee, D.; Yeo, J.; Yoo, J.H.; Allen, F.I.; Kim, E.; So, H.; Park, H.K.; Minor, A.M.; Grigoropoulos, C.P. Laser-induced reductive sintering of nickel oxide nanoparticles under ambient conditions. J. Phys. Chem. C 2015, 119, 6363–6372.
28. Nurfani, E.; Lailani, A.; Kesuma, W.A.P.; Anrokhi, M.S.; Kadja, G.T.M.; Rozana, M. UV sensitivity enhancement in Fe-doped ZnO films grown by ultrafast spray pyrolysis. Opt. Mater. 2021, 112, 110768.
29. Deka, B.K.; Hazarika, A.; Kim, J.; Jeong, H.E.; Park, Y.B.; Park, H.W. Fabrication of the piezoresistive sensor using the continuous laser-induced nanostructure growth for structural health monitoring. Carbon N. Y. 2019, 152, 376–387.

30. Henley, S.J.; Fryar, J.; Jayawardena, K.D.G.I.; Silva, S.R.P. Laser-assisted hydrothermal growth of size-controlled ZnO nanorods for sensing applications. Nanotechnology 2010, 21, 365502.
31. Yeasmin, M.; Das, T.; Baruah, S. Study on the hydrothermal growth of ZnO nanorods for piezotronic. ADBU J. Eng. Technol. 2019, 8, 1–5.
32. Samouco, A.; Marques, A.C.; Pimentel, A.; Martins, R.; Fortunato, E. Laser-induced electrodes towards low-cost flexible UV ZnO sensors. Flex. Print. Electron. 2018, 3, 044002.
33. Mai, H.H.; Tran, D.H.; Janssens, E. Non-enzymatic fluorescent glucose sensor using vertically aligned ZnO nanotubes grown by a one-step, seedless hydrothermal method. Microchim. Acta 2019, 186, 245.
34. Hu, J.; Zhang, M.; He, Y.; Zhang, M.; Shen, R.; Zhang, Y.; Wang, M.; Wu, G. Fabrication and potential applications of highly durable superhydrophobic polyethylene terephthalate fabrics produced by in-situ zinc oxide (ZnO) nanowires deposition and polydimethylsiloxane (pdms) packaging. Polymers 2020, 12, 2333.
35. Filip, A.; Musat, V.; Tigau, N.; Polosan, S.; Pimentel, A.; Ferreira, S.; Gomes, D.; Calmeiro, T.; Martins, R.; Fortunato, E. ZnO nanostructures grown on ITO coated glass substrate by hybrid microwave-assisted hydrothermal method. Optik 2020, 208, 164372.
36. Sanjeev, S.; Kekuda, D. Effect of annealing temperature on the structural and optical properties of zinc oxide (ZnO) thin films prepared by spin coating process. In IOP Conference Series: Materials Science and Engineering; IOP Publishing: Temple Circus Temple Way, Bristol, UK, 2015; Volume 73.
37. Kiriarachchi, H.D.; Abouzeid, K.M.; Bo, L.; El-Shall, M.S. Growth Mechanism of Sea Urchin ZnO Nanostructures in Aqueous Solutions and Their Photocatalytic Activity for the Degradation of Organic Dyes. ACS Omega 2019, 4, 14013–14020.
38. Pan, C.; Zhai, J.; Wang, Z.L. Piezotronics and Piezo-phototronics of Third Generation Semiconductor Nanowires. Chem. Rev. 2019, 119, 9303–9359.
39. Ghoderao, K.P.; Jamble, S.N.; Kale, R.B. Influence of pH on hydrothermally derived ZnO nanostructures. Optik 2018, 156, 758–771.
40. Young, S.-J.; Yang, C.-C.; Lai, L.-T. Review—Growth of Al-, Ga-, and In-Doped ZnO Nanostructures via a Low-Temperature Process and Their Application to Field Emission Devices and Ultraviolet Photosensors. J. Electrochem. Soc. 2017, 164, B3013–B3028.
41. Baruah, S.; Dutta, J. Hydrothermal growth of ZnO nanostructures. Sci. Technol. Adv. Mater. 2009, 10, 885–889.
42. Deka Boruah, B. Zinc oxide ultraviolet photodetectors: Rapid progress from conventional to self-powered photodetectors. Nanoscale Adv. 2019, 1, 2059–2085.

43. Jabeen, M.; Vasant Kumar, R.; Ali, N. A Review on Preparation of ZnO Nanorods and Their Use in Ethanol Vapors Sensing. Gas Sens. 2020, 1–24.
44. Hu, H.; Huang, X.; Deng, C.; Chen, X.; Qian, Y. Hydrothermal synthesis of ZnO nanowires and nanobelts on a large scale. Mater. Chem. Phys. 2007, 106, 58–62.
45. Eom, T.H.; Han, J.I. Single fiber UV detector based on hydrothermally synthesized ZnO nanorods for wearable computing devices. Appl. Surf. Sci. 2018, 428, 233–241.
46. Zhou, Q.; Xie, B.; Jin, L.; Chen, W.; Li, J. Hydrothermal Synthesis and Responsive Characteristics of Hierarchical Zinc Oxide Nanoflowers to Sulfur Dioxide. J. Nanotechnol. 2016, 2016, 6742104.
47. Türkyılmaz, Ş.Ş.; Güy, N.; Özacar, M. Photocatalytic efficiencies of Ni, Mn, Fe and Ag doped ZnO nanostructures synthesized by hydrothermal method: The synergistic/antagonistic effect between ZnO and metals. J. Photochem. Photobiol. A Chem. 2017, 341, 39–50.
48. Shivaraj, B.W.; Manjunatha, C.; Abhishek, B.; Nagaraju, G.; Panda, P.K. Hydrothermal synthesis of ZnO nanotubes for CO gas sensing. Sens. Int. 2020, 1, 100018.
49. Wu, H.; Ding, J.; Yang, D.; Li, J.; Shi, Y.; Zhou, Y. Graphene quantum dots doped ZnO superstructure (ZnO superstructure/GQDs) for weak UV intensity photodetector application. Ceram. Int. 2020, 46, 17800–17808.
50. Demes, T.; Ternon, C.; Riassetto, D.; Stambouli, V.; Langlet, M. Comprehensive study of hydrothermally grown ZnO nanowires. J. Mater. Sci. 2016, 51, 10652–10661.
51. Oh, D.K.; Choi, H.; Shin, H.; Kim, K.; Kim, M.; Ok, J.G. Tailoring zinc oxide nanowire architectures collectively by catalytic vapor-liquid-solid growth, catalyst-free vapor-solid growth, and low-temperature hydrothermal growth. Ceram. Int. 2021, 47, 2131–2143.
52. Alshehri, N.A.; Lewis, A.R.; Pleydell-Pearce, C.; Maffeis, T.G.G. Investigation of the growth parameters of hydrothermal ZnO nanowires for scale up applications. J. Saudi Chem. Soc. 2018, 22, 538–545.
53. Al-Hadeethi, Y.; Umar, A.; Ibrahim, A.A.; Al-Heniti, S.H.; Kumar, R.; Baskoutas, S.; Raffah, B.M. Synthesis, characterization and acetone gas sensing applications of Ag-doped ZnO nanoneedles. Ceram. Int. 2017, 43, 6765–6770.
54. Gao, W.; Li, Z. Nanostructures of zinc oxide. Int. J. Nanotechnol. 2009, 6, 245–257.
55. Yeo, J.; Hong, S.; Wanit, M.; Kang, H.W.; Lee, D.; Grigoropoulos, C.P.; Sung, H.J.; Ko, S.H. Rapid, one-step, digital selective growth of ZnO nanowires on 3D structures using laser induced hydrothermal growth. Adv. Funct. Mater. 2013, 23, 3316–3323.
56. Yeo, J.; Hong, S.; Kim, G.; Lee, H.; Suh, Y.D.; Park, I.; Grigoropoulos, C.P.; Ko, S.H. Laser-Induced Hydrothermal Growth of Heterogeneous Metal-Oxide Nanowire on Flexible Substrate by Laser Absorption Layer Design. ACS Nano 2015, 9, 6059–6068.

57. Kwon, J.; Hong, S.; Lee, H.; Yeo, J.; Lee, S.S.; Ko, S.H. Direct selective growth of ZnO nanowire arrays from inkjet-printed zinc acetate precursor on a heated substrate. Nanoscale Res. Lett. 2013, 8, 489.
58. Hong, S.; Yeo, J.; Manorotkul, W.; Kang, H.W.; Lee, J.; Han, S.; Rho, Y.; Suh, Y.D.; Sung, H.J.; Ko, S.H. Digital selective growth of a ZnO nanowire array by large scale laser decomposition of zinc acetate. Nanoscale 2013, 5, 3698–3703.
59. Amin, G.; Asif, M.H.; Zainelabdin, A.; Zaman, S.; Nur, O.; Willander, M. Influence of pH, precursor concentration, growth time, and temperature on the morphology of ZnO nanostructures grown by the hydrothermal method. J. Nanomater. 2011, 2011, 269692.
60. Nagpal, S.; Rahul, S.V.; Bhatnagar, P.K. Low cost UV sensor using ZnO nanorods on ITO electrodes. Eng. Res. Express 2020, 2, 025007.
61. Lu, C.; Qi, L.; Yang, J.; Tang, L.; Zhang, D.; Ma, J. Hydrothermal growth of large-scale micropatterned arrays of ultralong ZnO nanowires and nanobelts on zinc substrate. Chem. Commun. 2006, 2006, 3551–3553.
62. Uddin, A.S.M.I.; Yaqoob, U.; Phan, D.T.; Chung, G.S. A novel flexible acetylene gas sensor based on PI/PTFE-supported Ag-loaded vertical ZnO nanorods array. Sens. Actuators B Chem. 2016, 222, 536–543.
63. Tsay, C.Y.; Hsiao, I.P.; Chang, F.Y.; Hsu, C.L. Improving the photoelectrical characteristics of self-powered p-GaN film/n-ZnO nanowires heterojunction ultraviolet photodetectors through gallium and indium Co-doping. Mater. Sci. Semicond. Process. 2021, 121, 105295.
64. Lupan, O.; Magariu, N.; Khaledialidusti, R.; Mishra, A.K.; Hansen, S.; Krüger, H.; Postica, V.; Heinrich, H.; Viana, B.; Ono, L.K.; et al. Comparison of Thermal Annealing versus Hydrothermal Treatment Effects on the Detection Performances of ZnO Nanowires. ACS Appl. Mater. Interfaces 2021, 13, 10537–10552.
65. Wahid, K.A.; Lee, W.Y.; Lee, H.W.; Teh, A.S.; Bien, D.C.S.; Azid, I.A. Effect of seed annealing temperature and growth duration on hydrothermal ZnO nanorod structures and their electrical characteristics. Appl. Surf. Sci. 2013, 283, 629–635.
66. Babapour, A.; Yang, B.; Bahang, S.; Cao, W. Low-temperature sol-gel-derived nanosilver-embedded silane coating as biofilm inhibitor. Nanotechnology 2011, 22, 155602.
67. Wu, W.; He, Q.; Jiang, C. Magnetic iron oxide nanoparticles: Synthesis and surface functionalization strategies. Nanoscale Res. Lett. 2008, 3, 397–415.